Title	Stochastic backward/forward sweep power flow analysis for islanded microgrids
Author(s)	Subramanian, Lalitha; Gooi, Hoay Beng
Citation	Subramanian, L., & Gooi, H. B. (2018). Stochastic Backward/Forward Sweep Power Flow Analysis for Islanded Microgrids. 2018 IEEE PES Innovative Smart Grid Technologies, ISGT 2018, 48-53. doi:10.1109/ISGT-Asia.2018.8467763
Date	2018
URL	http://hdl.handle.net/10220/46121
Rights	© 2018 IEEE. Personal use of this material is permitted. Permission from IEEE must be obtained for all other uses, in any current or future media, including reprinting/republishing this material for advertising or promotional purposes, creating new collective works, for resale or redistribution to servers or lists, or reuse of any copyrighted component of this work in other works. The published version is available at: [https://dr.ntu.edu.sg/handle/10220/46121].

Stochastic Backward/Forward Sweep Power Flow Analysis for Islanded Microgrids

Lalitha Subramanian
Energy Research Institute at NTU,
Nanyang Technological University, Singapore.

H B Gooi
School of Electrical and Electronic Engineering,
Nanyang Technological University, Singapore.

***Abstract*—Distributed generation-based islanded microgrids lack a constant reference voltage node, making it difficult to compute the power flows in the microgrid using traditional power system analysis tools. In this work, we model the droop equations that allow voltage and frequency regulation among the distributed sources in the backward/forward sweep algorithm. As a result, the system frequency is one of the unknown state variables that has to be computed by power flow analysis. Since the backward/forward sweep algorithm is primarily applied only to radial distribution systems, the algorithm is then modified to extend its applicability to weakly-meshed microgrid topologies. The distributed generation units are modelled as solar generation with their uncertainties defined by Beta distribution while the load uncertainties are modelled using normal distribution. Finally, a stochastic islanded microgrid power flow tool is developed using the polynomial chaos approximation technique.**

***Index Terms*—Chaos function, Hermite polynomial, radial, stochastic, weakly-meshed.**

I. Introduction

WITH the rapid growth of the renewable energy industry, the trend of realizing small independent power systems called microgrids is on the rise. Islanded microgrids based on converter-based distributed generation (DG) systems do not possess a fixed voltage reference node. In [1], the authors have showed that the parallel operation of inverters in an isolated system may be solved by modelling the droop relations between the active power - frequency (Pf) and the reactive power - voltage (Qv) relations. This results in the addition of a new state variable: frequency, to the problem [2]. Power flow analysis tools are employed to obtain the steady state variables of a power system, which includes the system voltages and frequency in the case of an islanded microgrid.

A. Deterministic Power Flow Analysis of Islanded Microgrids

Various established techniques such as Gauss-Seidel, Newton-Raphson, and fast-decoupled methods may be employed to solve the power flow problem in well-meshed transmission power systems. The Jacobian matrix may be ill-conditioned or singular for radial and weakly-meshed power systems. Hence, derivative-based techniques may not serve as reliable power flow analysis tools for microgrids. In [3], the authors have developed a power flow analysis tool based on the Newton trust region method for islanded microgrids (IMGs). The droop equations of the microgrid have been incorporated into the power flow equations and solved using the Newton-Raphson power flow in [4]. However, this method is only suited for a well-meshed microgrid and may result in singular Jacobian matrices when applied to radial and weakly-meshed microgrids [5].

In this paper, we apply a backward/forward sweep (BFS) algorithm based on the direct approach described in [6]. The method involves the formation of two simple matrices based on the system topology: the nodal injection-nodal current matrix (BIBC) and the nodal current-nodal voltage matrix (BCBV), that eliminate the time-consuming decomposition and the backward/forward substitution of the Y matrix in the power flow algorithm. This step greatly simplifies the computation steps in the algorithm and enhances its time efficiency [6]. The inverter control is modelled by the droop equations [1] and are incorporated in the BFS algorithm in this work. Since the BFS algorithm is only suited for radial distribution systems, it has to be modified for its applicability to weakly-meshed microgrids. To facilitate this, we modify the BIBC and BCBV matrices of the BFS algorithm.

B. Stochastic Power Flow Analysis of Islanded Microgrids

Stochastic factors such as the load and renewable generation uncertainties may not be ignored as they become significant in smaller power systems like the microgrids. Moreover, as the microgrid operation is mainly dependent on DGs in IMGs, their uncertainties will have to be taken into account in power systems stability and security studies [7]. In this work, we extended the BFS-based IMG power flow tool to work in the stochastic domain, i.e. by modelling the uncertainties in the system. The stochastic power flow analysis (SPFA) yields each of the state variables and dependent variables of the system as a probability density function (PDF). Probabilistic power flow methods may be mainly classified into Monte Carlo Simulation (MCS) [8], analytical methods such as cummulant method (CM) [9] and approximation methods such as the '2m' and '3m' point estimate methods (PEMs) [10]. MCS requires several thousands of deterministic power flow analysis (DPFA) runs with random samples generated from the probability distributions of the input variables to maintain a high accuracy [8]. The CM uses cummulants of the input variables to computes the cummulants of the state variables.

Series expansions such as the Gram-Charlier and Cornish-Fisher series are used to obtain the PDFs of the state variables in CM and PEM techniques [11]. The main limitation of using

the series expansions is that their convergence cannot always be guaranteed [12]. In this work we utilize a polynomial chaos expansion (PCE) based on the Hermite polynomials described in [12] to approximate the deterministic BFS by a polynomial stochastic surface. The principle of this method is that the computationally intensive deterministic runs of the power flow analysis may be replaced by a set of polynomial calculations, thus reducing the computational complexity. As the number of stochastic variables in the system increases, the computation time of the MCS also increases exponentially. The computation time requirement for the same accuracy will be far lesser than the MCS due to the polynomial approximation of the stochastic response surface (SRS) method.

C. Paper Organization

Section II describes the BFS method with the additional inverter droop control equations incorporated in them. Section III presents the modification in the BFS matrices to extend its applicability to both radial and weakly-meshed microgrids. The stochastic variables of the microgrid are modelled to formulate the SRS in section IV. Section V presents a kernel density estimation technique from which the PDFs of the output variables are estimated along with the results obtained for a 33-bus microgrid. Section VI presents the overall contributions of the work and its future scope.

II. Modified BFS with Droop Equations for Radial Microgrids

For a microgrid operating in the grid-connected mode, the BFS power flow does not pose any problem as there is a stiff node that acts as a voltage reference. However, in the islanded mode, both active and reactive powers are shared by the generators according to their respective droop function, which allows variation of the node voltages and the system frequency. The state variable vector includes the nodal voltage magnitudes, voltage angles, and the system frequency. They are to be computed by the power flow algorithm as described below.

Step 1: The entries of the nodal voltage vector V are assumed to be 1 per unit and the frequency deviation from the nominal value Δf is assumed to be zero at the start. Steps 3 to 10 form the inner frequency droop control loop, while the voltage of the reference node is adjusted according to the reactive power imbalance in the outer voltage droop control in step 2.

Step 2: The change in the DG reactive power is computed by the reactive power - voltage (Qv) droop equation given by (1).

$$\Delta Q_{g_i} = \frac{|V_i| - 1}{n_{Q_i}}, \quad \forall i \varepsilon Gen. \tag{1}$$

Step 3: The change in the DG active power is computed by the active power - frequency (Pf) droop equation given by (2). Based on the changes in the active and reactive power calculated, the complex power injected at each node is calculated by (3), where $P^0_{g_i}$ and $Q^0_{g_i}$ are the rated active and reactive power of the DGs at the rated frequency f^0 and rated voltage V^0_i respectively.

$$\Delta P_{g_i} = \frac{\Delta f}{m_{P_i}}, \forall i \varepsilon Gen. \tag{2}$$

$$S_i = P_{l_i} + P^0_{g_i} + \Delta P_{g_i} + j * \left(Q_{l_i} + Q^0_{g_i} + \Delta Q_{g_i}\right) \tag{3}$$

Step 4: The node current vector I may be calculated using (4), where S_i is the complex power injected into the i^{th} node.

$$I_i{}^k = \left(\frac{S_i}{V_i{}^k}\right)^* \tag{4}$$

Step 5: The branch current vector I_{branch} may be computed with the help of $[BIBC]$ as shown in (5).

$$I_{branch} = [BIBC] I_{node} \tag{5}$$

$[BIBC]$ may be formed offline, as it remains the same for a specific system topology. The steps for the formation of $[BIBC]$ are given below:

1) Create a matrix of zeroes of size $M * N$, where M is the number of branches and N is the number of nodes in the microgrid.
2) If the k^{th} line is located between the i^{th} node and the j^{th} node, copy the i^{th} column to the v column of the matrix and fill the element $BIBC(k, j)$ with 1.
3) Repeat the previous step for each of the lines in the radial microgrid.

Step 6: The reference node or node 1 is the gateway for the excess or deficit power transfer. Thus the power traded at the first node is indicative of the system frequency [5]. The change in the system frequency according to (6).

$$\Delta f = -m_{P_1}\left[P_{L^1} + P^0_{G_1} + Re\left(\sum_{i \epsilon A_1} V_1 I^*_{1i}\right)\right] \tag{6}$$

Step 7: The system frequency is modified according to the change in the frequency calculated in the previous step as in (7). Equation (8) modifies the line impedance vector according to the new frequency, where X_{ij} is the line reactance at the rated frequency.

$$f = f^0 + \Delta f \tag{7}$$

$$Z_{ij} = R_{ij} + jX_{ij}\frac{f}{f^0} \tag{8}$$

Step 8: Compute $[BCBV]$ and $[\Delta V]$ given by (9) and (10) respectively, where Z_{branch} is the branch impedance vector that changes with the system frequency.

$$[BCBV] = [BIBC] * diag(Z_{branch}) \tag{9}$$

$$\Delta V = [BCBV] I_{branch} \tag{10}$$

Step 9: Compute the updated nodal voltage of each node except node 1, based on (11)

$$V_i = V^0 - \Delta V_i \tag{11}$$

Step 10: Repeat steps 3 to 9 until the node voltages converge to a steady value. In this work, the tolerance criteria given by

(12) is checked between the last two successive iterations of nodal voltage values. k indicates the current iteration number of the inner loop.

$$min\left(V_i^k - V_i^{k-1}\right) < \epsilon, \forall i = 2, \ldots, N \tag{12}$$

Step 11: The outer loop voltage droop control equations are modelled in (13) and (14), where the voltage of the first node is altered based on the reactive power trading of the node.

$$\Delta V^0 = -m_{Q_1}\left[Q_{L1} + Q_{G_1}^0 + Im\left(\sum_{i\epsilon A_1} V_1 I_{1i}^*\right)\right] \tag{13}$$

$$V^0 = \begin{bmatrix}1 & \ldots & 1\end{bmatrix}_{1*N}^T - \begin{bmatrix}\Delta V_0 & \ldots & \Delta V_0\end{bmatrix}_{1*N}^T \tag{14}$$

Step 12: If the voltage of the first node has not converged to a steady value, repeat from step 2. The convergence of the first node voltage can be checked by the tolerance criteria given in (15) where p indicates the current iteration number of the outer loop.

$$min\left(V_1^p - V_1^{p-1}\right) < \epsilon \tag{15}$$

III. Modification for Weakly-meshed Topologies

The matrices BIBC and BCBV that were described in the last section will have to be modified for weakly-meshed systems. High density load areas in the distribution system are often the nodes that are involved in the meshed topologies [6]. Normally open tie-switches may be closed on high-loading periods of these nodes. The presence of meshes do not affect the nodal current vector but increases the size of the branch current vector. The tie branches that convert the system from a radial to the weakly meshed system are identified separately.

The BIBC matrix formation steps are described in step 5 of the BFS algorithm in the previous section. Once the radial system branches are added, the tie branches may be added to the BIBC matrix. If the k^{th} branch is a tie branch between the i^{th} node and the j^{th} node, fill in the elements of the k^{th} column by subtracting the elements of the j^{th} from the i^{th} column. Also, fill the element $BIBC(k,k)$ with 1 [6]. The BIBC matrix can thus be computed offline based on the system topology.

The BCBV matrix may be obtained by the modified BIBC matrix and the new line impedance vector appended with the tie line impedances as shown in (9). For obtaining the change in the nodal voltages, (10) may be replaced by (16), where the BIBV matrix is given by (17) and (18). Except for the changes in the matrix formations and (10), all other steps in the algorithm are valid for weakly-meshed microgrids.

$$[\Delta V] = [BIBV][I] \tag{16}$$

$$[BCBV][BIBC] = \begin{bmatrix}A & M^T\\ M & N\end{bmatrix} \tag{17}$$

$$[BIBV] = [A - M^T N^{-1} M] \tag{18}$$

IV. Stochastic Response Surface Formulation

This section describes the transformation of the deterministic power flow analysis to the stochastic domain. The principle used in this method is to formulate a polynomial surface representing the function of variation of each state variable in terms of the stochastic input variables of the system [8]. Once the stochastic polynomial response surface is formulated for each response variable, it simply replaces the deterministic BFS by the computation of a set of polynomials. The formulation of SRS that represents the BFS is described in this section.

The stochastic input variables include the active power generation of the DGs, active power, and reactive power demands of the load. In this study, the IEEE 33-bus distribution system is considered with five solar photovotaic DGs at nodes 1, 6, 13, 25, and 33 [13]. The photovoltaic generation is influenced by the variation of the sunlight intensity which is often described by the Beta distribution considering a short time scale of hours or days [14]. From (19) we can infer that if the solar irradiation is modelled by a Beta distribution, the active power output of the PV system is also given by a Beta distribution, where r is the solar irradiation; A is the area of the battery; and η is the battery efficiency. The PDF of the Beta distribution is given by (20). The Beta parameters (a, b) and the maximum irradiation r_{max} are given by the solar irradiation forecasts. Then the active power output of the i^{th} DG, P_{g_i}, is given in (20) by replacing r and r_{max} with P and P_{max} respectively.

$$P = rA\eta \tag{19}$$

$$f(r) = \frac{\Gamma(\alpha+\beta)}{\Gamma(\alpha)\Gamma(\beta)}\left(\frac{r}{r_{max}}\right)^{\alpha-1}\left(1 - \frac{r}{r_{max}}\right)^{\beta-1} \tag{20}$$

The load demand uncertainties are usually modelled by the Normal distribution function, with the means μ_p and μ_q and standard deviations σ_2^p and σ_2^q from the load forecasts. The PDFs of the Normal distribution function is given by (21).

$$f(P_l) = \frac{1}{\sqrt{2\pi}\sigma_p} e^{\frac{(P_l-\mu_p)^2}{2\sigma_2^p}}; f(Q_l) = \frac{1}{\sqrt{2\pi}\sigma_q} e^{\frac{(Q_l-\mu_q)^2}{2\sigma_2^q}} \tag{21}$$

Consider the problem of formulation of a SRS for each output response variable y. The polynomial chaos function of the output response variable in terms of the stochastic input vector X may be written as shown in (22), where the X denotes the vector of stochastic input variables as given in (23); n denotes the number of stochastic input variables; the coefficients a_{j_i} denote the unknown coefficients of the polynomial that have to be computed; and the H_m function denotes the Hermite polynomial expansion of m^{th} order. Hermite polynomials are specifically used to represent the polynomial expansion when each of the stochastic variable follows a standard Normal

distribution. The Hermite polynomial function is defined by (24).

$$y = a_0 + \sum_{j_1=1}^{n} a_{j_1} H_1(x_1) + \sum_{j_1=1}^{n} \sum_{j_2=1}^{j_1} a_{j_1 j_2} H_2(x_1, x_2) + \sum_{j_1=1}^{n} \sum_{j_2=1}^{j_1} \sum_{j_3=1}^{j_2} a_{j_1 j_2 j_3} H_3(x_1, x_2, x_3) + \dots \quad (22)$$

$$X = [x_1, x_2, \dots, x_n]^T \quad (23)$$

$$H_m(x_1, x_2, \dots, x_n) = (-1)^m e^{\frac{1}{2} X^T X} \frac{\partial^n}{\partial x_1 .. \partial x_n} e^{-\frac{1}{2} X^T X} \quad (24)$$

The higher the order of the Hermite polynomial expansion considered, the higher is the accuracy of the stochastic model. In this work, we consider a Hermite polynomial expansion of the second order. Accordingly, (22) can be reduced to (25). The total number of unknown coefficients to be computed for a polynomial chaos expansion of the m^{th} order with n stochastic input variables is given by (26).

$$y = a_0 + \sum_{j_1=1}^{n} a_{j_1} x_{j_1} + \sum_{j_1=1}^{n} a_{j_1 j_1} (x_{j_1}^2 - 1) + \sum_{j_1=1}^{n} \sum_{j_2=j_1+1}^{n} a_{j_1 j_2} x_{j_1} x_{j_2} \quad (25)$$

$$n_a = \frac{(n+m)!}{n!m!} \quad (26)$$

It is to be noted that each of the desired output response variable is modelled by a different polynomial. If Y represents the vector of the desired response variables, then it may be represented by (27), where r is the number of output responses that require the formulation of polynomial approximation models. Y may include the state variables such as the node voltage magnitudes, node voltage angles, or other dependent variables like the line flows, total active power loss, etc. Thus, the unknown coefficient matrix for the entire Y vector may be represented by A defined in (28).

In order to compute the n_a unknown coefficients for each response y, n_a linearly independent equations are required. They can be generated as in (29), where the H is the stochastic input Hermite matrix defined in (30) and $Y1$ is the overall response matrix that can be filled with all the r response values obtained from each of the n_a runs of the deterministic power flow with n_a sets of samples of the stochastic input variables. The $Y1$ matrix may be formulated as shown in (31).

$$Y = [y_1, y_2, \dots, y_r]^T \quad (27)$$

$$A = \begin{bmatrix} a_0^1 & .. & a_0^r \\ [a_1^1, a_2^1, \dots, a_n^1]^T & .. & [a_1^r, a_2^r, \dots, a_n^r]^T \\ [a_{11}^1, a_{22}^1, \dots, a_{nn}^1]^T & .. & [a_{11}^r, a_{22}^r, \dots, a_{nn}^r]^T \\ [a_{12}^1, a_{13}^1, \dots, a_{1n}^1]^T & .. & [a_{12}^r, a_{13}^r, \dots, a_{1n}^r]^T \\ [a_{23}^1, \dots, a_{2n}^1]^T & .. & [a_{23}^r, \dots, a_{2n}^r]^T \\ \dots & .. & \dots \\ [a_{(n-1)(n)}^1]^T & .. & [a_{(n-1)(n)}^r]^T \end{bmatrix} \quad (28)$$

$$Y1 = H * A \quad (29)$$

$$H = \begin{bmatrix} 1, x_{11}..x_{1n}, (x_{11}^2 - 1).., (x_{11}x_{12})..(x_{1(n-1))}x_{1n}) \\ 1, x_{21}..x_{2n}, (x_{21}^2 - 1).., (x_{21}x_{22})..(x_{2(n-1))}x_{2n}) \\ .... \\ .... \\ 1, x_{r1}..x_{rn}, (x_{r1}^2 - 1).., (x_{r1}x_{r2})..(x_{r(n-1))}x_{rn}) \end{bmatrix} \quad (30)$$

$$Y1 = [Y_1 Y_2 \dots Y_{n_a}] \quad (31)$$

The n_a different sets of the stochastic input samples are known as the collocation points (CPs) and are used for the response surface formulation. It is to be noted that the n_a linearly independent sets of stochastic input samples are required to solve the unknown coefficients. The CPs will have to be chosen carefully to ensure the correctness of the polynomial model. In this work, we utilize the efficient CP selection method for the standard Normal distribution proposed in [15]. The CPs are the most influencing sample points of the standard Normal distribution that affect the stochastic variation of the output response and are chosen according to the rules listed below.

1) The sample points close to the origin are the most preferred as it is the region of highest probability for the standard Normal distribution.
2) The sample points picked must be symmetric with respect to the origin to examine the response surface variation with different directions [15].
3) Few random samples may be chosen to improve the model robustness.
4) Samples from the region of very low probability are generally avoided or restricted to one or two CPs [15].

The CPs chosen for the deterministic runs are in the standard Normal distribution, whereas the stochastic inputs in the BFS power flow problem follow the Beta and Normal distribution. Thus, the collocation points chosen according to [15] are converted to their respective distributions by the transformation equation (32), where $F(x)$ is the probability density function of the Beta or Normal distribution for the DG power outputs and the load powers respectively.

$$SV_i = F_i^{-1} \left(\frac{1}{\sqrt{2\pi}} \int_{-\infty}^{x_i} e^{-\frac{t^2}{2}} dt \right) \quad (32)$$

With the values of the stochastic variable samples SV_i, the BFS deterministic power flow described in the previous section is run n_a times with the different set of sample inputs. $Y1$ is filled with the values of the output variables after the deterministic runs and the unknown coefficients are obtained by solving (29). Thus, the approximate polynomial stochastic response surface has been formulated and so, the deterministic runs of the power flow may be replaced by the computation of the set of polynomials.

A. Probability Density Estimation

Once the set of polynomial equivalents for the power flow are obtained, similar to the ideal MCS technique, the response

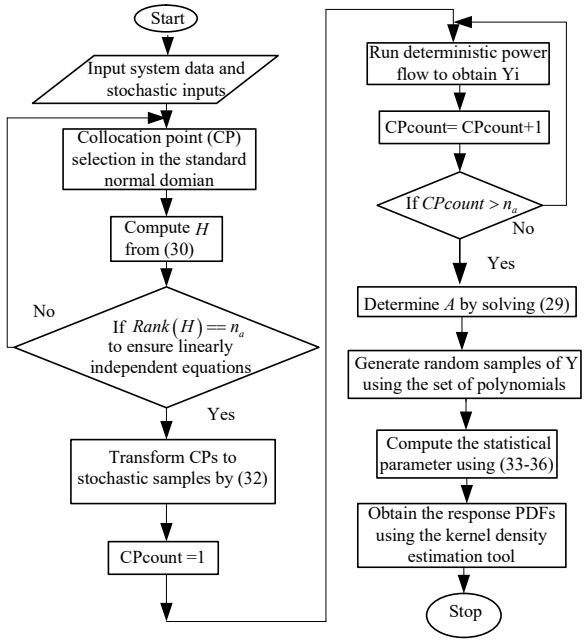

Fig. 1. Flowchart of the stochastic power flow tool

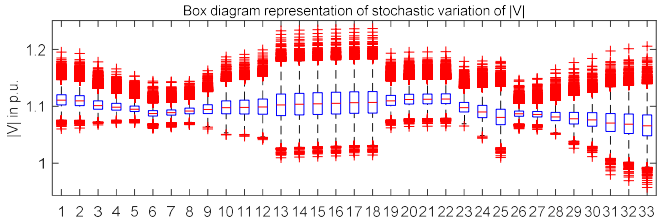

Fig. 2. Stochastic variation of node voltage magnitudes

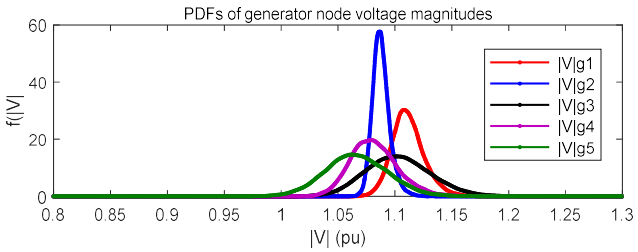

Fig. 3. PDFs of DG node voltages

variables for a large number of random samples may be computed using the polynomial in a very less computation time as shown in section V. Thus, the response surface formulation reduces the computation time, while maintaining the accuracy of the MCS. With the response variable outputs for a large number of samples, the statistical parameters such as the mean, variance, skewness, and kurtosis may be determined for each response variable using (33), (34), (35), and (36) respectively.

$$\mu(y_i) = \frac{1}{r} \sum_{j=1}^{n_{sample}} y_{ij} \tag{33}$$

$$\sigma^2(y_i) = \frac{1}{r} \sum_{j=1}^{n_{sample}} (y_{ij} - \mu(y_{ij}))^2 \tag{34}$$

$$\gamma_1(y_i) = \frac{1}{r\sigma^3(y_i)} \sum_{j=1}^{n_{sample}} (y_{ij} - \mu(y_{ij}))^3 \tag{35}$$

$$\gamma_2(y_i) = \frac{1}{r\sigma^4(y_i)} \sum_{j=1}^{n_{sample}} (y_{ij} - \mu(y_{ij}))^4 \tag{36}$$

The PDFs and CDFs of the response variable distributions may be obtained using the kernel density estimation tool in MATLAB from the obtained sample responses. The overall flowchart of the steps involved in the stochastic power flow tool is presented in figure 1.

V. Simulation Results and Inferences

The IEEE 33-bus distribution system is considered as an islanded microgrid with five DGs at nodes 1, 6, 13, 25, and 33 with droop coefficients -0.05, -1, -0.1, -1, and -0.2 p.u. respectively. The nominal active and reactive power generated by the DGs are considered to be 0.9 and 0.6 p.u. [5]. The system data along with the DG data may be obtained from [5]. The power flow analysis results obtained with this data, using the droop-based BFS power flow described in section II is presented in table I under the radial system column. Since the power flow algorithm was modified to extend its applicability to weakly-meshed topologies, we consider that the Normally-open tie lines between nodes 8-21, 9-15, 12-22, 18-33, and 25-29 are closed. The line impedance data of the tie-lines considered in this work may be obtained from [13]. The results obtained from the generalized power flow algorithm is shown in table I under the weakly-meshed system column.

Considering the DG active power outputs to be stochastic variables that follow Beta distribution with parameters α and β as 2.06 and 2.5 respectively; and the load active and reactive powers to follow Normal distribution with mean values as that of the original data and a standard deviation of 5% [12], the SRS algorithm described in section IV is used to obtain the probability distribution of the state and dependent variables of the microgrid. The statistical parameters of the nodal voltage magnitudes are obtained and plotted as a box diagram shown in figure 2. Using the kernel density estimation tool of MATLAB, the PDFs of the voltage magnitudes of the DG buses is plotted in 3. The accuracy and computation time comparison between the MCS and the proposed method is presented in table II. The comparison verifies that the stochastic response surface method (SRSM) lessens the computational burden of conventional stochastic computation, while maintaining the accuracy of the MCS.

VI. Conclusion and Future Scope

In this work, a stochastic droop-based BFS power flow analysis tool has been developed specifically for the IMGs, which include both radial and weakly-meshed grid topologies.

TABLE I
33-BUS MICROGRID - DROOP-BASED BFS POWER FLOW RESULTS

Node	Radial System		Weakly-Meshed System	
	$\|V\|$ in p.u.	δ in deg	$\|V\|$ in p.u.	δ in deg
1	0.9964	0.0000	0.9980	0.0000
2	0.9972	0.0047	0.9989	0.0053
3	1.0000	0.0270	1.0018	0.0175
4	1.0009	0.0137	1.0028	0.0308
5	1.0013	0.0024	1.0035	0.0472
6	1.0022	-0.0150	1.0051	0.0900
7	1.0026	0.0331	1.0050	0.1431
8	1.0026	0.0522	1.0046	0.1478
9	1.0008	0.0679	1.0021	0.1293
10	0.9984	0.0761	0.9996	0.0490
11	0.9980	0.0838	0.9992	0.0430
12	0.9970	0.1006	0.9983	0.0334
13	0.9914	0.0790	0.9919	-0.0414
14	0.9935	0.1465	0.9935	0.0007
15	0.9948	0.1786	0.9945	0.0063
16	0.9960	0.1984	0.9951	0.0324
17	0.9979	0.2634	0.9957	0.1351
18	0.9985	0.2714	0.9957	0.1507
19	0.9978	0.0155	0.9994	0.0217
20	1.0013	0.0819	1.0029	0.1385
21	1.0020	0.1009	1.0036	0.1731
22	1.0026	0.1208	1.0042	0.2431
23	1.0013	0.0752	1.0027	0.0220
24	1.0030	0.1789	1.0037	0.0372
25	1.0016	0.2405	1.0015	0.0108
26	1.0029	-0.0420	1.0060	0.0812
27	1.0037	-0.0804	1.0071	0.0684
28	1.0074	-0.2041	1.0127	0.0340
29	1.0097	-0.3070	1.0166	-0.0011
30	1.0102	-0.3761	1.0175	-0.0718
31	1.0075	-0.3759	1.0157	-0.0921
32	1.0061	-0.3917	1.0147	-0.1160
33	1.0036	-0.4542	1.0125	-0.1910
	P_g in p.u.	Q_g in p.u.	P_g in p.u.	Q_g in p.u.
1	2.4641	0.9728	2.4701	0.9402
6	0.9782	0.8978	0.9785	0.8949
13	1.6821	0.9858	1.6851	0.9813
25	0.9782	0.8984	0.9785	0.8985
33	1.2910	0.8820	1.2925	0.8373
	P_{loss} in p.u.	Q_{loss} in p.u.	P_{loss} in p.u.	Q_{loss} in p.u.
	0.0364	0.0368	0.0253	0.0468

TABLE II
COMPARISON OF THE PERFORMANCE OF SRSM AND MCS

Ideal accuracy - MCS $n_{sample} = 20000$		
Method	Maximum error in %	CPU time (s)
SRSM $n_{sample} = 10000$	0.23	1.5543
SRSM $n_{sample} = 20000$	0.09	4.1527
MCS $n_{sample} = 10000$	0.15	95.1728

The uncertainties of the renewable generation and the loads have been modelled and accounted for in the analysis. The proposed tool has been validated against the ideal MCS. It has been verified that the computational efficiency has improved while retaining the accuracy of the power flow results. This tool can find applications in solving computationally complex power system analysis problems like contingency analysis, security-constrained optimal power flow and stability analysis in the stochastic domain. The correlation between the stochastic variables will be modelled in the future version of the tool. The performance of the SRS algorithm may be compared with other analytical methods like the cummulant and PEM methods in terms of accuracy and computational efficiency.

ACKNOWLEDGEMENT

The authors would like to thank the Energy Research Institute at NTU, Singapore, for the financial support provided to carry out this work.

REFERENCES

[1] M. C. Chandorkar, D. M. Divan, and R. Adapa, "Control of parallel connected inverters in standalone ac supply systems," *IEEE Transactions on Industry Applications*, vol. 29, no. 1, pp. 136–143, 1993.

[2] G. Diaz, J. Gomez-Aleixandre, and J. Coto, "Direct Backward/Forward Sweep Algorithm for Solving Load Power Flows in AC Droop-Regulated Microgrids," *IEEE Transactions on Smart Grid*, vol. 7, no. 5, pp. 2208–2217, 2016.

[3] M. M. A. Abdelaziz, H. E. Farag, E. F. El-Saadany, and Y. A. R. I. Mohamed, "A novel and generalized three-phase power flow algorithm for islanded microgrids using a newton trust region method," *IEEE Transactions on Power Systems*, vol. 28, no. 1, pp. 190–201, 2013.

[4] F. Mumtaz, M. H. Syed, M. A. Hosani, and H. H. Zeineldin, "A Novel Approach to Solve Power Flow for Islanded Microgrids Using Modified Newton Raphson with Droop Control of DG," *IEEE Transactions on Sustainable Energy*, vol. 7, no. 2, pp. 493–503, 2016.

[5] F. Hameed, M. A. Hosani, and H. H. Zeineldin, "A Modified Backward/Forward Sweep Load Flow Method for Islanded Radial Microgrids," *IEEE Transactions on Smart Grid*, vol. PP, no. 99, pp. 1–9, 2017.

[6] J. H. Teng, "A direct approach for distribution system load flow solutions," *IEEE Transactions on Power Delivery*, vol. 18, no. 3, pp. 882–887, 2003.

[7] V. Mohan, R. Suresh, J. G. Singh, W. Ongsakul, and N. Madhu, "Microgrid Energy Management Combining Sensitivities, Interval and Probabilistic Uncertainties of Renewable Generation and Loads," *IEEE Journal on Emerging and Selected Topics in Circuits and Systems*, vol. 7, no. 2, pp. 262–270, 2017.

[8] Y. Li, W. Li, W. Yan, J. Yu, and X. Zhao, "Probabilistic optimal power flow considering correlations of wind speeds following different distributions," *IEEE Transactions on Power Systems*, vol. 29, no. 4, pp. 1847–1854, 2014.

[9] M. Fan, V. Vittal, G. T. Heydt, and R. Ayyanar, "Probabilistic power flow studies for transmission systems with photovoltaic generation using cumulants," *IEEE Transactions on Power Systems*, vol. 27, no. 4, pp. 2251–2261, 2012.

[10] X. Ai, S. Member, and J. Wen, "A Discrete Point Estimate Method for Probabilistic Load Flow Based on the Measured Data of Wind Power," *IEEE Transactions on Industry Applications*, vol. 49, no. 5, pp. 2244–2252, 2013.

[11] S. J. Yao and W. Yan, "Cornish-Fisher Expansion for Probabilistic Power Flow of the Distribution System with Wind Energy System," in *4th International Conference on Electric Utility Deregulation and Restructuring and Power Technologies*, 2011, pp. 1378–1383.

[12] Z. Ren, W. Li, R. Billinton, and W. Yan, "Probabilistic Power Flow Analysis Based on the Stochastic Response Surface Method," *IEEE Transactions on Power Systems*, vol. 31, no. 3, pp. 2307–2315, 2016.

[13] M. E. Baran and F. F. Wu, "Network reconfiguration in distribution systems for loss reduction and load balancing," *Power Delivery, IEEE Transactions on*, vol. 4, no. 2, pp. 1401–1407, 1989.

[14] S. Tian and H. Wang, "Probabilistic Load Flow Analysis Considering the Correlation for Microgrid with Wind and Photovoltaic System," in *5th International Conference on Electric Utility Deregulation and Restructuring and Power Technologies*, no. 1, 2015, pp. 2003–2008.

[15] S. Isukapalli and P. G. Georgopoulos, "Computational methods for sensitivity and uncertainty analysis for environmental and biological models," *National Exposure Research Laboratory, US Environmental Protection Agency*, vol. 600, no. 1, p. 68, 2001.